第 34 卷第 4 期
2015 年 8 月

红 外 与 毫 米 波 学 报
J. Infrared Millim. Waves

Vol. 34, No. 4
August, 2015

文章编号: 1001 - 9014(2015)04 - 0427 - 05

DOI:10.11972/j.issn.1001 - 9014.2015.04.008

Avalanche characterization of high speed single-photon detector based on InGaAs/InP APD

LI Yong-Fu[1*], LIU Jun-Liang[1,2], WANG Qing-Pu[1], FANG Jia-Xiong[1]

(1. Advanced Research Center for Optics, Shandong University, Jinan 250100, China;
2. School of Information Science and Technology, Shandong University, Jinan 250100, China)

Abstract: A 1.25-GHz high speed short-wavelength infrared single-photon detector (SPD) based on InGaAs/InP avalanche photodiode (APD) 1.25-GHz sine wave gating and Bessel LC low-pass filters (LPFs) was described. The avalanche signal amplitude distributions of the SPD at different reverse DC biases are studied experimentally by adjusting the discrimination level of the comparator circuit. As the discrimination level is raised, both detection efficiency and dark count rate reduce exponentially, while the after-pulse probability firstly rises to a peak value and then reduces. It indicates that the discrimination level should be as low as possible to obtain better SPD performance.

Key words: InGaAs/InP APD, single-photon detector, short-wavelength infrared
PACS: 85.30.De, 85.60.Dw, 85.60.Gz

基于 InGaAs/InP 雪崩光电二极管的高速单光子探测器雪崩特性研究

李永富[1*], 刘俊良[1,2], 王青圃[1], 方家熊[1]
(1. 山东大学 光学高等研究中心,山东 济南 250100;
2. 山东大学 信息科学与工程学院,山东 济南 250100)

摘要:报道了一种基于 InGaAs/InP 雪崩光电二极管、1.25 GHz 正弦波门控及贝塞尔低通滤波器的 1.25 GHz 高速短波红外单光子探测器.通过调整比较电路的鉴别电平,实验研究了单光子探测器雪崩信号幅度随反向直流偏压的变化.随着鉴别电平的提高,单光子探测器的探测效率及暗计数率均呈指数衰减,而后脉冲概率先增大到一个峰值,然后减小.研究表明,为获得更高的性能,需要尽量降低单光子探测器的鉴别电平.

关 键 词:InGaAs/InP 雪崩光电二极管;单光子探测器;短波红外

中图分类号:TN215 **文献标识码**:A

Introduction

Short-wavelength infrared single-photon detector based on Geiger InGaAs/InP APD has been used widely in quantum key distribution (QKD)[1-5], and has urgent requirements in long distance laser radar system[6-7] due to its high detection efficiency, compactness, high reliability, low power consumption, cryo-cool-free working condition, etc. Therefore, InGaAs/InP based SPDs have been a hot spot of research for years. However, InGaAs/InP SPDs also suffer from significant after-pulsing due to charge traps, which generally limit them to gated-mode operation. Under such condition, the detector could detect the photon signal only when the gate is on. To meet actual application requirements, various researches have been carried out to improve the performance of the SPDs, for example, to suppress the after-pulse by using different biasing and quenching techniques[2,8-11], to increase the code rate with higher gating frequency[4, 12-15], etc. But up to now, the highest detection efficiency reported for gated-mode InGaAs/InP APD based SPDs is 50% at 1310 nm at the cost of dark count rate up to 7×10^{-5}/gate and after-pulse up to 6.4%[14]. Nevertheless, little work refers to the distribution characteristics of avalanche signal of APD based SPD.

In this paper, we demonstrate a 1.25 GHz sine wave gated InGaAs/InP SPDs with simple inductance-ca-

Received date: 2015 - 02 - 01, **revised date**: 2015 - 06 - 18 **收稿日期**:2015 - 02 - 01, **修回日期**:2015 - 06 - 18
Foundation items: Supported by Independent Innovation Foundation of Shandong University(2014YE015)
Biography:李永富(1983-),男,山东潍坊人,博士,主要从事光电传感器件的研究及应用工作
* **Corresponding author**: E-mail: yfli@sdu.edu.cn

pacitance (LC) low-pass filters (LPFs). The avalanche distributions of the SPD are characterized experimentally. And the detection efficiency, dark count rate and after-pulse probability versus the comparator threshold of the discrimination circuit are studied. For InGaAs/InP SPD with sine wave gate, as the comparator threshold is raised, both detection efficiency and dark count rate reduce exponentially, while the after-pulse probability rises firstly to a peak value and then reduces.

1 Experimental setup

The single-photon detector (SPD) is designed based on PGA-300 type InGaAs/InP APD (Princeton Lightwave), 1.25 GHz pseudo-sine wave gating, 3 stages of 9th Bessel LPFs, 2 stages of high-gain low-noise broadband amplifiers (LNA) and an adjustable high-speed comparator (CMP). The SPD is shown in Fig. 1. The APD is mounted on a copper heat sink and is cooled to -48℃ by a 4-stage TEC module. The 1.25 GHz sine wave is generated from a commercial signal generator and is amplified to 11.27 $V_{p\text{-}p}$ by a 1 W medium-power amplifier. The DC bias and the gating signal are both applied on the APD through an improved gated-passive-quenching-circuit (GPQC), which has been introduced in our previous work[16].

As shown in Fig. 1, the output signal of the APD passes through 3 stages of LPFs and two stages of amplifiers. Three LPF with -3dB bandwidth of 550 MHz can adequately suppress the transient response noise of the APD by 60 dB. An inexpensive broadband amplifier SGA4563Z is chosen for the amplifier with gain as high as 25 dB at 1 GHz and noise figure as low as 1.9 dB. One amplifier is inserted between each two LPFs. And then a high-speed adjustable comparator is used to normalize the amplitude of the amplified avalanche pulse. The pulse shaping circuit extends the pulse width to 5 ns for data acquisition, which is completed by an FPGA based data acquisition board.

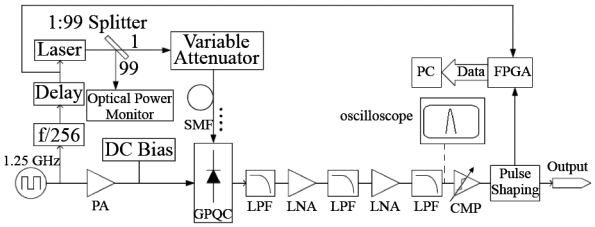

Fig. 1 System configuration for 1.25 GHz gated SPD and peripheral equipments for test. PA: 1W medium-power RF amplifier. LPF: 9th Bessel low pass filter. LNA: high-gain low-noise broadband amplifier. CMP: high-speed adjustable comparator. GPQC: gated passive quenching circuit. SMF: single mode fiber

图1 1.25 GHz门控单光子探测器系统及外围测试装置图,PA为1 W中功率射频放大器,LPF为9阶贝塞尔低通滤波器,LNA为高增益低噪声宽带放大器,CMP为高速可调比较器,GPQC为门控被动猝灭电路,SMF为单模光纤

A faint-laser single-photon source is used to test the performance of single-photon detectors. The 1.25-GHz gating signal is divided by 256 to trigger a pulsed diode laser PicoQuant PDL 800-B with 1550 nm wavelength. The laser pulse has typically 30 ps pulse width that yields smaller timing jitter. The laser is divided into two parts by a 1:99 beam splitter, the 99/100 part is used to monitor the optical power with EXFO PM-1600, and the 1/100 part is connected to a variable attenuator EXFO FVA-3150 to attenuate furthermore. In order to lower the possibility that one pulse contains multiple photons, the laser is attenuated to the degree that the per pulse photon number is 0.1 on average. Such single-photon signal is transmitted to the pig-tailed APD through one single-mode fiber. The performance of the detector is usually characterized by dark-count rate, detection efficiency and after-pulse probability. Several kinds of equations have been used to calculate those characteristics, corresponding to different definitions and conditions. We choose those that are suitable for high-frequency gated SPDs.

The average dark-count rate per gate is used to evaluate the dark-count rate of the SPD. The average dark-count rate per gate I_{dark} is given by

$$I_{\text{dark}} = \frac{C_{\text{dark}}}{f} \quad , \quad (1)$$

where C_{dark} is the number of count per second when the laser is off, and f is the gating frequency.

The detection efficiency of the SPD is the probability that one arrived photon generate a detectable avalanche pulse. Considering Poisson distribution, the detection efficiency η can be calculated by

$$\eta = \frac{1}{\mu}\ln\left(\frac{1 - I_{\text{dark}}}{1 - I_{\text{ph}}}\right) \quad , \quad (2)$$

where $I_{\text{ph}} = C_{\text{ph}}/f_{\text{L}}$, C_{ph} is the count events per second in the illuminated gates when the laser is on, f_{L} is the laser frequency that is 1/256 of the gating frequency f, and μ is the mean photon number per laser pulse and $\mu = 0.1$ here.

The after-pulse probability is usually defined as the probability that one previous photon-induced pulse generate one or more non-photon-induced pulses subsequently due to the emission of carriers that were trapped in deep-levels during previous photon-induced avalanche process[14].

Corresponding to the definition above, we use the following equation

$$P_{\text{ap}} = \frac{I_{\text{NI}} - I_{\text{dark}}}{I_{\text{ph}} - I_{\text{NI}}} \times \frac{f}{f_{\text{L}}} \quad , \quad (3)$$

where $I_{\text{NI}} = C_{\text{NI}}/(f\text{-}f_{\text{L}})$, C_{NI} is the count per second in the non-illuminated gates when the laser is on. All count events are counted by two gated counters implemented in the FPGA and sent to the PC to complete the calculation.

2 Results and discussion

We obtained the avalanche waveforms distribution at different reverse DC biases using an oscilloscope DSO-X-91604A with 16 GHz bandwidth, as shown in Fig. 2. In the measurements, the SPD was illuminated in every 256th gate, and the reverse DC bias (V_{bias}) was adjusted from 62.56 to 63.34 V. With increasing V_{bias}, the avalanche signal amplitude shows overall trend of increase.

And the amplitude of the avalanche signal varies greatly. As V_{bias} increases from 62.56 to 63.34 V, the avalanche pulse amplitude distribution range increase from 42 - 450 mV to 42 - 900 mV. Meanwhile, the number of pulses after the main pulse distribution region also increase, which usually contain both dark count and after-pulses.

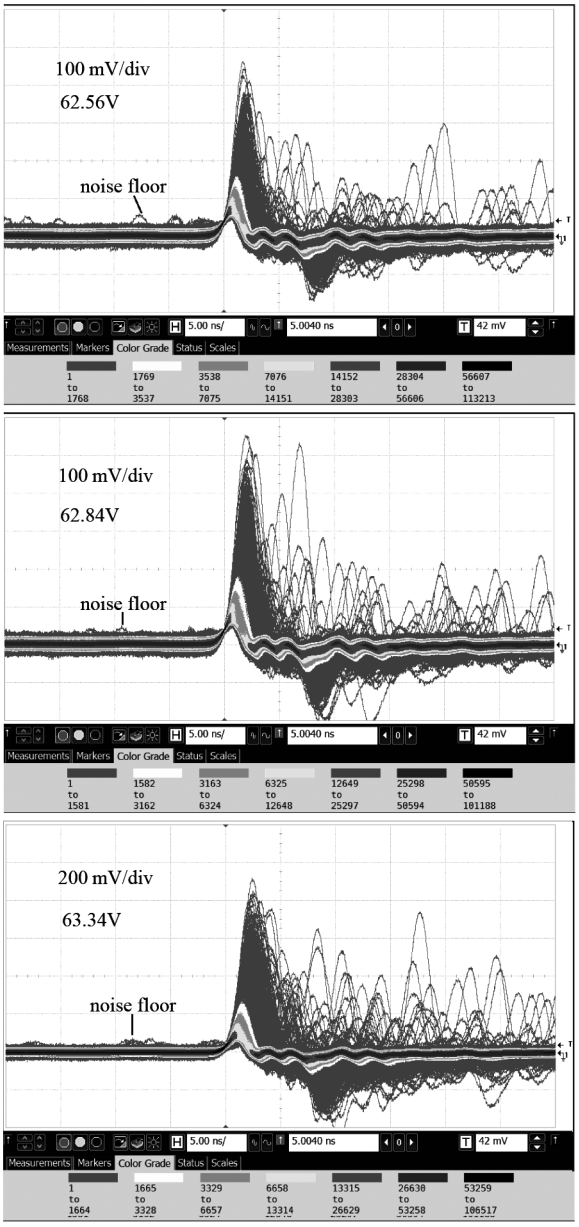

Fig. 2　Avalanche waveforms distribution at different reverse DC biases

图 2　不同反向直流偏压下雪崩波形分布

In order to further study the avalanche pulse, the amplitude distribution characteristics of count in non-illuminated gate (C_{NI}), dark count (C_{dark}) and photon count in illuminated gate (C_{ph}) under different V_{bias} were studied by adjusting the discrimination level of the comparator. The results are shown in Fig. 3. C_{NI}, C_{dark} and C_{ph} show similar exponential decay distribution as discrimination level increase. C_{NI}, C_{dark} and C_{ph} reduce more quickly with discrimination level under lower V_{bias}. The results indicate that the ratio of high-amplitude avalanche pulse increase with V_{bias}.

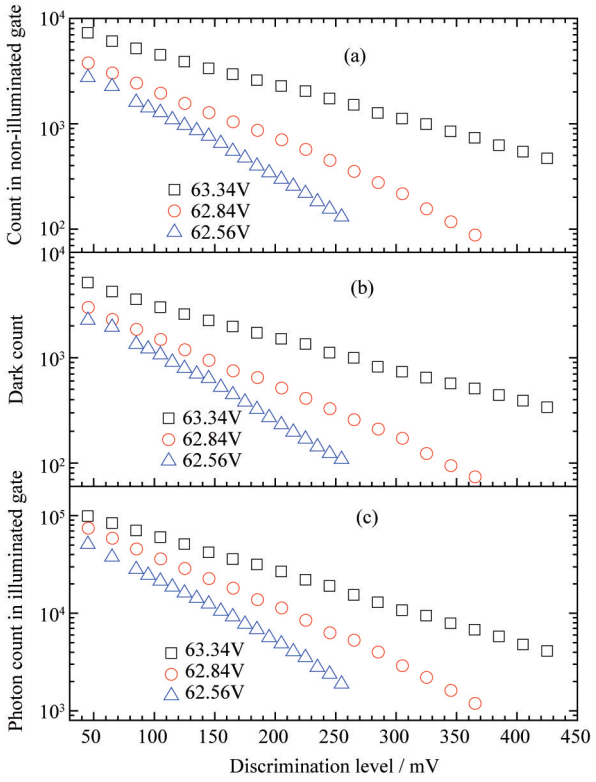

Fig. 3　Count in non-illuminated gate (C_{NI}) (a) Dark count (C_{dark}) (b) and Photon count in illuminated gate (C_{ph}) (c) versus discrimination level of the comparator under different V_{bias}

图 3　不同直流偏压下(a)无光门内计数(C_{NI})，(b) 暗计数(C_{dark})以及(c)有光门内光计数(C_{ph})随鉴别电平的变化

Figure 4 and Fig. 5 show that the detection efficiency and dark count rate reduce exponentially under different V_{bias}, respectively. The photon-induced avalanche pulses have similar amplitude distribution with the non-photon-induced avalanche pulses for the SPD with sine wave gating. These results are slightly different to those of Alessandro Restelli et al. [14], in which the avalanche amplitude of the SPD with Gaussian gating has a Gaussian distribution. This suggests that the avalanche amplitude decay is closely related to the gating waveform, and that the shape of gating signal has influence on the SPD performance.

Because almost each of the faint-laser pulses contains one photon or less on average, each photon-induced avalanche event can be mostly attributed to one photon-induced carrier. Considering the similar amplitude distribution between the photon-induced avalanche pulses and the non-photon-induced avalanche pulses, it can be inferred that both dark count and photon count result from one carrier, that is, one thermal carrier for one dark count and one photon-induced carrier for one photon count.

Figure 6 shows the after-pulse probability versus

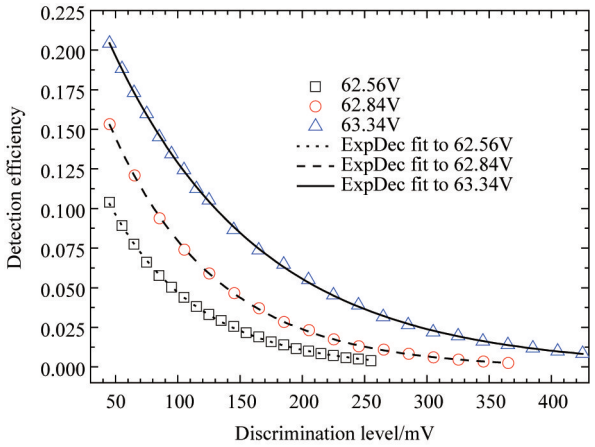

Fig. 4 Detection efficiency versus discrimination level of the comparator under different V_{bias}

图 4 不同直流偏压下系统探测效率随鉴别电平的变化

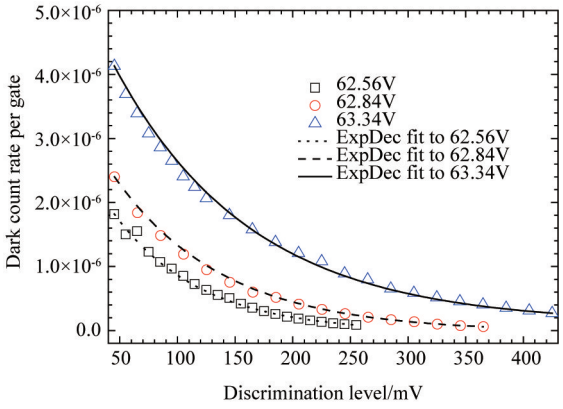

Fig. 5 Dark count rate versus discrimination level of the comparator under different V_{bias}

图 5 不同直流偏压下暗计数率随鉴别电平的变化

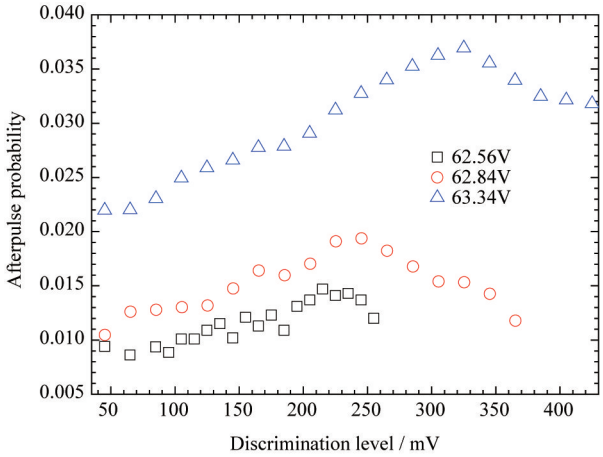

Fig. 6 After-pulse probability versus discrimination level of the comparator under different V_{bias}

图 6 不同直流偏压下后脉冲概率随鉴别电平的变化

discrimination level of the comparator under different V_{bias}. With the discrimination level increasing from the noise floor, the after-pulse probability firstly increased to a peak value and then reduced. Such tendency became more obvious with V_{bias} raised from 62.56 V to 63.34 V. The after-pulse probability is calculated from equation (3). Considering the measurements in Fig. 2, with the increase of V_{bias}, the avalanche signal amplitude shows overall trend of increase. As shown in Fig. 7, both the amplitude and the count in non-illuminated gates increase with V_{bias}. This suggests that an avalanche pulse with larger amplitude is more probable to be followed by an after-pulse. One possible explanation for this is that the avalanche pulse with larger amplitude involves with more carriers, which may be trapped by the generation-recombination center in the interface of the APD, increasing the possibility to trigger an after-pulse in the following gate.

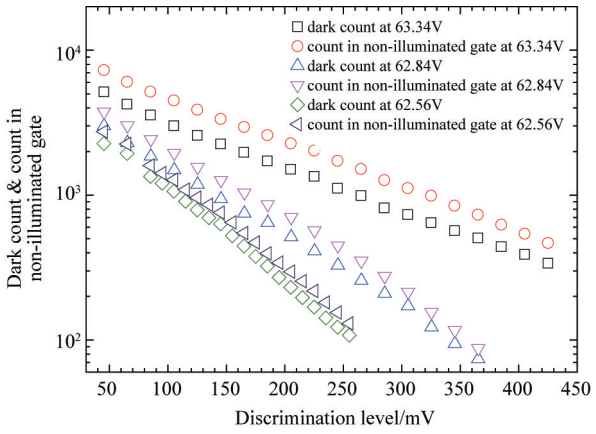

Fig. 7 Comparison between C_{NI} and C_{dark} under different V_{bias}

图 7 不同直流偏压下无光门内计数 C_{NI} 及暗计数 C_{dark} 的对比

As for the peak in each curve in Fig. 6, one possible explanation is that after-pulses result mostly from more than one trapped carrier. In the previous avalanche, multiple carriers are trapped and then released simultaneously in the following gate, triggering an avalanche pulse with larger amplitude than typical avalanches. As the discrimination level is increased, both photon count and dark count reduce more quickly than after-pulse, and thus, after-pulse probability increases firstly. And compared to the photon-induced carriers and thermal carriers that result from the whole thick absorption layer, most of the trapped carriers concentrate in the deep-levels of the APD and trigger avalanches with relatively smaller amplitude variation. Consequently, as the discrimination level is raised further, after-pulse probability reduces.

3 Conclusion

In conclusion, we demonstrate a 1.25 GHz sine wave gated InGaAs/InP SPD with simple LC LPFs. The avalanche distribution of the SPD is characterized experimentally. The detection efficiency, dark count rate and after-pulse probability versus the comparator threshold of the discrimination circuit are studied. As the discrimination level is raised, both detection efficiency and dark

count rate reduce exponentially, while the after-pulse probability firstly rise to a peak value and then reduce. The results indicate that the discrimination level of the SPD should be as low as possible to obtain better performance. And when the discrimination level is near the noise floor, the detection efficiency, dark count rate and after-pulse probability are 20.4%, 4.1×10^{-6}/gate and 2%, respectively.

References

[1] Dixon A R, Yuan Z L, Dynes J F, *et al*. Gigahertz decoy quantum key distribution with 1 Mbit/s secure key rate [J]. *Optics Express*, 2008, **16**(23): 18790-18979.

[2] Nambu Y, Takahashi S, Yoshino K, *et al*. Efficient and low-noise single-photon avalanche photodiode for 1.244-GHz clocked quantum key distribution [J]. *Optics Express*, 2011, **19**(21): 20531-20541.

[3] Yuan Z L, Dlxon A R, Dynes J F, *et al*. Practical gigahertz quantum key distribution based on avalanche photodiodes [J]. *New Journal of Physics*, 2009, **11**: 045019-1-11.

[4] Zhang J, Eraerds P, Wanlenta N, *et al*. 2.23 GHz gating InGaAs/InP single-photon avalanche diode for quantum key distribution [J]. *Proc. SPIE*, 2010, 7681: 76810Z.

[5] Namekata N, Takesue H, Honjo T, *et al*. High-rate quantum key distribution over 100 km using ultra-low-noise, 2-GHz sinusoidally gated InGaAs/InP avalanche photodiodes [J]. *Optics Express*, 2011, **19**(11): 10632-10639.

[6] Yang F, Zhang X, He Y, *et al*. Laser raging system based on high speed pseudorandom modulation and photon counting techniques [J]. *Chinese Journal of Lasers*, 2013, **40**(2): 184-188.

[7] Min R, Gu X R, Liang Y, *et al*. Laser ranging at 1550 nm with 1 GHz sine-wave gated InGaAs/InP APD single-photon detector [J]. *Optics Express*, 2011, **29**(14): 13497-13502.

[8] Namekata N, Mori S, Inoue S. Quantum key distribution over an installed multimode optical fiber local area network [J]. *Optics Express*, 2005, **13**(25): 9961-9969.

[9] Dlxon A R, Yuan Z L, Dynes J F, et al. Continuous operation of high bit rate quantum key distribution [J]. *Applied Physics Letters*, 2010, **96**(16): 161102.

[10] Yuan Z L, Sharpe A W, Dynes J F, *et al*. Multi-gigahertz operation of photon counting InGaAs avalanche photodiodes [J]. *Applied Physics Letters*, 2010, **96**(7): 071101.

[11] Bethune D S, Risk W. An auto compensating fiber-optic quantum cryptography system based on polarization splitting of light [J]. *J. Sel. Top. Quant. Phys.*, *IEEE Trans.*, 2000, **36**(3): 340-347.

[12] Namekata N, Adachi S, Inoue S. 1.5 GHz single-photon detection at telecommunication wavelengths using sinusoidally gated InGaAs/InP avalanche photodiode [J]. *Optics Express*, 2009, **17**(8): 6275-6282.

[13] Liang X L, Jiang W H, Liu J H, *et al*. A 1.25 GHz InGaAs/InP single-photon detector for high-speed quantum cryptography [J]. *Chinese Journal of Lasers*, 2012, **39**(8): 0818001.

[14] Restelli A, Bienfang J C, Migdall A L. Single-photon detection efficiency up to 50% at 1310 nm with an InGaAs/InP avalanche diode gated at 1.25 GHz [J]. *Applied Physics Letters*, 2013, **102**: 141104.

[15] Huang J H, Wu G, Zeng H P. Study of 1.5 GHz harmonics ultra-short pulse gated InGaAs/InP avalanche photodiode single-photon detection [J]. *Acta Optica Sinica*, 2014, **34**(2): 0204001-1-5.

[16] Li Y F, Liu J L, Wang Q P, *et al*. High speed single-photon detector based on simple LC filter [J]. *Acta Optica Sinica*, 2013, **33**(B12), 7-11.